Ultra-Compact Graphene-Embedded Optical Phase Modulators

Ran Hao[1], Jia-Min Jin[1], and Er-Ping Li[1]*

[1*] Department of Information Science & Electronic Engineering, Zhejiang University, Hangzhou, Zhejiang, China.
rhao@zju.edu.cn

Abstract

Optical modulator is the key components in the optical communication, yet the low modulation efficiency limits its development. A high efficiency, ultra-compact optical modulator is proposed which the electro-refraction effect has been significantly enhanced. The different kinds of graphene schemes are compared and discussed. A graphene embedded Mach-Zender modulator has been theoretically demonstrated with the advantage of ultra-compact footprint ($4\times30\ \mu m^2$), high modulation efficiency (20 V·μm), fast modulation speed and large extinction ratio (35dB). Our results may promote various on-chip active components, boosting the utilization of graphene in optical applications.

1. Introduction

Optical modulator is the key component in on-chip interconnection and integrated optoelectronic circuits [1]. The operation mechanisms can be divided into two kinds: A change in the real part of the refractive index caused by the applied voltage is known as the electro-refraction (ER) effect, whereas a change in the imaginary part of the refractive index is known as the electro-absorption (EA) effect [1]. Nevertheless, these two effects are too weak in pure silicon at the communication wavelengths so that it usually needs an extremely large arm length to reach the required modulation, e. g., a recent 50 Gbit/s Mach-Zehnder modulator has the length of 1 millimeter [2]. The large footprint of optical modulator makes it impossible to be integrated into a single chip. Driven by next generation on-chip communication, minimizing the size and improving the efficiency of modulator is of vital importance.

2. Graphene's Optical Property

Graphene, the two-dimensional (2D) carbon sheet in honeycomb lattice with only one-atom-layer thickness has attracted lots of interest due to its remarkable mechanical, electric, magnetic thermal and optical properties[3]. Graphene provides the highest carrier mobility that is much larger than silicon's capable, and much stronger interaction with light for the electro-refractive or electro-absorptive effects in a broad frequency regime [4-5], which make it an excellent material for the high performance optical modulator. Additionally, the conductivity of graphene can be modified by means of chemical doping, electric field, or magnetic fields [1]. In the mid-infrared wavelengths, when graphene is doped with a certain electron or hole concentration [6-7], it is demonstrated both theoretically [8] and experimentally [9] that graphene surface plasmons (GSP) can exist. Graphene is an excellent platform for plasmonic devices owing to its large active-control of its conductivity-function that is not seen in noble metals [6]. The conductivity of graphene can be modified by means of chemical doping, electric field, or magnetic fields following the Kubo formula. The imaginary part of graphene conductivity can attain negative and positive values in different ranges of frequencies depending on the level of chemical potential. The complex conductivity of a free-standing isolated graphene shows regions of frequencies and chemical potentials for which $\sigma_{g,i} < 0$, whereas for other regions $\sigma_{g,i} > 0$. Since Graphene's periodicity is in the two-dimensional lattice plane, it reveals anisotropic material properties: the in-plane permittivity ($\varepsilon_{//}$) can be actively tuned by the chemical potentials (the Fermi level), whereas the out-of-plane permittivity ($\varepsilon_{\perp}$, in the direction perpendicular to the graphene sheet) does not vary with the external parameters and stays constant at 2.5. Fig. 1 shows the in-plane conductivity σ and the permittivity of an infinite graphene sheet calculated from the Kubo formula at the wavelength λ=1550 nm.

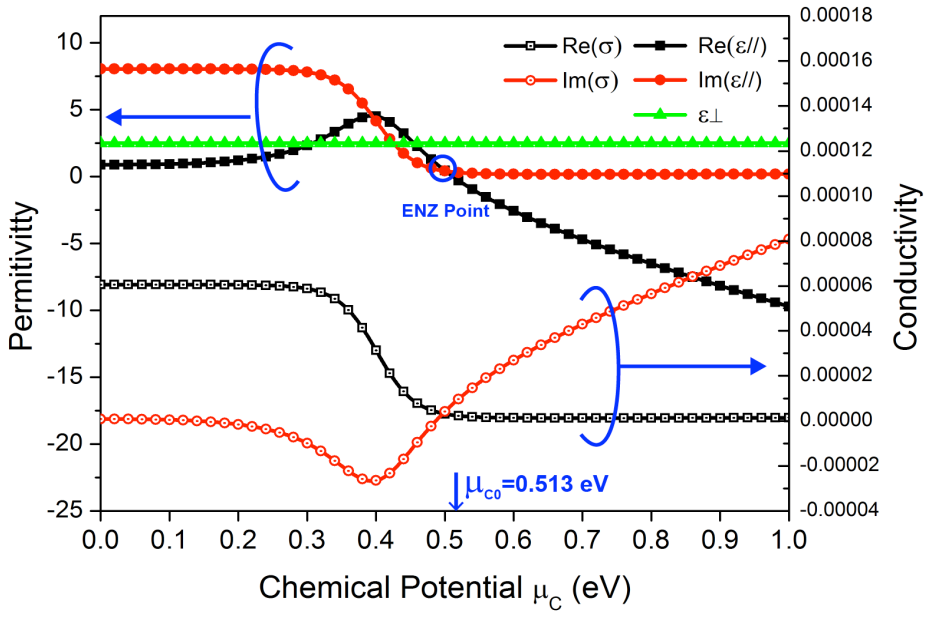

FIG. 1. The conductivity and permittivity of an infinite graphene sheet (the wavelength is fixed at 1550 nm).

3. The Mach-Zehnder Phase modulator

Since a waveguide tends to concentrate light in the center, a silicon waveguide with eight layers of graphene embedded silicon waveguide (GESW) is considered to maximize the graphene-light interaction, as shown in Fig. 2(a). Fig.2 (b) depicts the corresponding effective index variation regarding the to graphene's chemical potential. The n_{eff} of the proposed waveguide is lower than silicon's refractive index (3.45) at all chemical potentials. And an inflection point is observed in the Re(n_{eff}) curve at μ_C=0.4 eV, where n_{eff} changes intensively near the inflection point. After μ_C=0.4 eV, Re(n_{eff}) gradually deceases and Im(n_{eff}) stay constant.

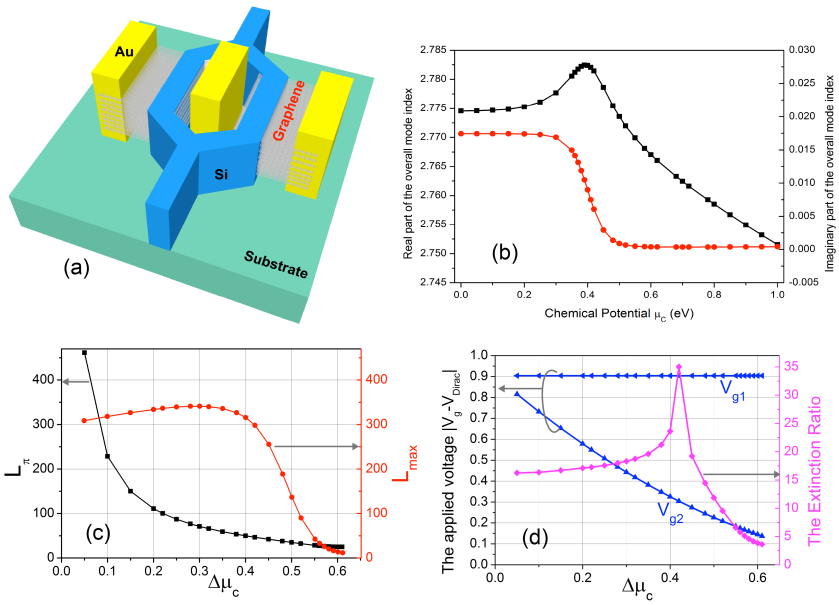

Fig.2 (a) The schematic pictures for eight-layer graphene embedded MZ modulator configuration, (b) the corresponding electric field distribution in one of the arm, (c) the relationship between Lπ/Lmax and $\Delta\mu_C$, (d) the relationship between the applied votages/extinction ratio and $\Delta\mu_C$.

The impressive value of large Δn_{eff} is appreciated for the modulators based on ER effect, such as Mach-Zehnder (MZ) modulator, as shown in the schematic picture of Fig. 2 (a). Let us first fix one chemical potential μ_{C1} =1 eV due to the smallest Im(n_{eff}), then sweep the other chemical potential μ_{C2} from 0.39 eV to 0.95 eV according to the

linear portion of the black curve in Fig. 2 (b). With μ_{C2} changes, the corresponding Δn_{eff} will be modified, thus the required arm length L_π to reach the π phase shift is modified. L_π can be calculated through $\pi = \Delta n_{eff} \times L_\pi$. Fig. 2 (c) has shown the relationship between Lπ and $\Delta\mu_C$ while μ_{C1} is fixed at 1 eV. The general trend is that L_π becomes smaller with the increase of $\Delta\mu_C$, but after $\Delta\mu_C$ is increased to 0.3 eV, the decrease of Lπ is quite limit. Of course, for MZ modulator, the smaller L_π is, the better footprint will be. But Lπ cannot be infinitely small, there is a restrict condition that the corresponding propagation loss must be in acceptable range. The propagation loss can be evaluated in terms of the maximum allowed length L_{max} as shown in the red curve in Fig. 2 (c), indicating the length where the energy at the output decays to 1/e of its original value. We would focus our attention on the condition that $L_\pi < L_{max}$ in which case the waveguide has enough power at the output. Under this restriction, the smallest L_π is 27.57 μm when $\Delta\mu_C$=0.56 eV, which is two orders of magnitude smaller than the present reported value [2]. If the width of the modulation arm is 450 nm and the distance between the two arms is 1.1 μm, taking into account of the electrode width of 1 μm on each arm side, the overall width of the device is 4 μm, thus the footprint of our proposed modulator is only 30×4 μm^2. Note conventional MZ modulator needs several millimeters to reach the π phase shift. This small size as well as the CMOS compactable structure indicates its valuable capability to be integrated into photonic circuits in a single chip. For the proposed MZI modulator, the two arms are applied with different voltages: one is with the constant voltage V_{g1} which corresponds to μ_{C1} =1 eV, thus it is called the reference arm; the other is switched between V_{g1} (for signal "1") and V_{g2} (for signal "0") according to the transmitted signals, thus it is called the modulated arm. The blue curves in Fig. 2 (d) have shown the calculated applied voltages for the modulated arm, which are much smaller if compared with other modulators. The difference between V_{g1} and V_{g1} is called π shift voltage V_π. As expected, V_π increases when $\Delta\mu_C$ is enlarged. The product between L_π and V_π is known as the modulation efficiency. Since L_π decreases much faster than the increase speed of V_π, the minimum $V_\pi L_\pi$ would be achieved at 20 V·μm when L_π is smallest at 27.57 μm. The purple curve in Fig. 2 (d) shows the relationship between the extinction ratio and ΔV_g, where a maximum extinction ratio of 35 dB has been observed at $\Delta\mu_C$ =0.42 eV. The obtained high extinction ratio is due to the Im(n_{eff}) have taken the same value under the two modulation states.

4. Comparison between various graphene sheets

To further improve the modulation efficiency, let us compare different kinds of graphene sheet. Instead to insert graphene sheets individually with interval space, it is also possible to employ a N-layer thick graphene sheet. To simplify the comparison, N=2 is compared here. The real part of the index (Re(n_{eff})) and the imaginary part of the index (Im(n_{eff})) for the proposed waveguide under the chemical potential from 0eV to 1eV is shown as Fig.3 (a) and Fig.3(b), including the black circle line (monolayer GESW), blue square line (two separated monolayer GESW), and red triangle line (bi-layer GESW). The corresponding electric field distributions have been also plotted in Fig. 3(c), Fig.3 (d) and Fig.3 (e), for the monolayer GESW, two separated monolayer GESW, bi-layer GESW, respectively. The variation of Re(n_{eff}) for the bi-layer embedded waveguide is roughly two times of the monolayer embedded structure as expected. However, the variation of Re(n_{eff}) for the bi-layer GESW is much larger than that of the two separated monolayer graphene embedded, which implies the light-matter interaction between light and bi-layer graphene is much more pronounced compared to that of the two separated monolayer graphene. This implies that better modulation efficiency can be achieved if N-layer thick graphene is embedded. Secondly, these three curves have basically the same variation trend, namely, it first increases to a maximum value (around the chemical potential of 0.4eV) and then decreases to the minimum value (at the chemical potential of 1eV). Therefore, a large Δn_{eff} can be obtained when chemical potential is between 0.4eV and 1eV. In addition, due to graphene is a highly tunable material, its chemical potential (the Fermi level) can be varied with the applied gate-voltage. As a result, one could generate the desired phase by easily control the applied gate-voltage.

Although it has better performance, there are two issues need to be clarify when dealing with N-layer thick graphene sheet. As experimentally verified in Ref.[10], the N value cannot be larger than 5. When the number of layer N<5 (called few-layer graphene), the conductivity of N-layer structure is N times of monolayer graphene's conductivity: $\sigma_N = N \times \sigma_0$ [9-10]. On the other hand, the effective thickness of N-layer structure is $d_N = N \times d_0$ [9-10]. As a result, the in-plane permittivity of few-layer graphene can be also obtained from the Kubo formula. Moreover, It should be also mentioned that the carrier mobility of few-layer graphene is slower if compared to the monolayer graphene. Because the resistance and response time of the proposed modulator are proportional to the carrier mobility, the slower carrier mobility in our proposed few-layer GESW will reduce the modulation speed and increase the energy consumption compared to the monolayer GESW.

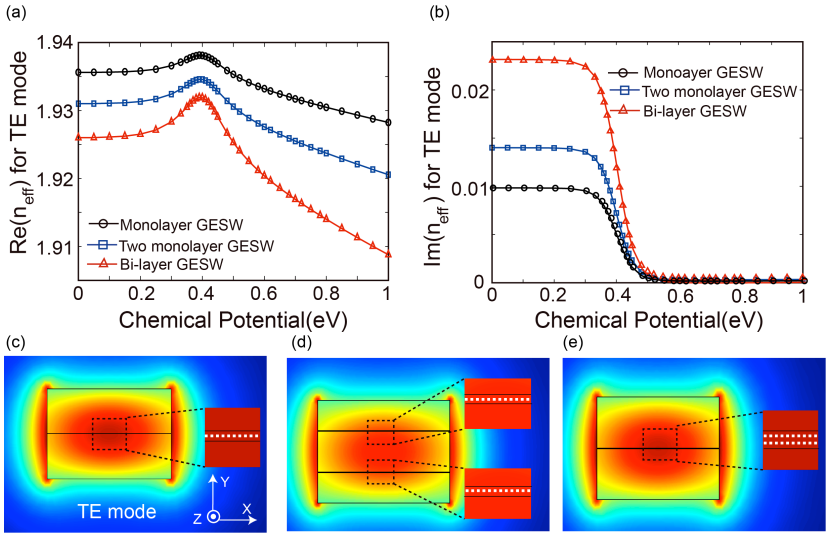

Fig.3 (a) the Re(n_{eff}) with chemical potential variation for monolayer, two separated monolayer, and bi-layer GESW; (b) the Im(n_{eff}) with chemical potential variation for monolayer, two separated monolayer, and bi-layer GESW; (c) (d), (e) represents the electric field distribution for TE polarization mode of monolayer, two separated monolayer, and bi-layer GESW under chemical potential of 0eV, respectively.

5. Conclusion

In conclusion, by embedding the graphene sheet into the silicon waveguide, the light-matter interaction has been significantly enhanced. An eight-layer graphene sheets embedded modulator has been proposed based on this effect, with the advantage of ultra-compact footprint (30×4 μm^2), short arm length (27.57 μm), low drive voltage, high modulation efficiency (20 V·μm), large modulation bandwidth, as well as high extinction ratio. The different graphene sheets are compared when embedding them in the silicon waveguide. The proposed graphene modulator has great potentials for future active components, showing significant influence for optical interconnects in future integrated optoelectronic systems. The flexibility of graphene sheets may enable radically different photonic devices. The high modulation efficiency as well as ultrafast speed modulation suggests the valuable perspective for utilizing graphene optics in nanophotonic circuits.

6. Acknowledgments

This work was supported by the National Natural Science Foundation of China (61205054), and the Excellent Young Faculty Awards Program (Zijin Plan) at Zhejiang University.

7. References

1. Q. Bao and K. P. Loh, "Graphene Photonics, Plasmonics, and Broadband Optoelectronic Devices," *ACS Nano*, *Volume 6*, 2012, pp. 3677-3694.
2. D. J. Thomson, F. Y. Gardes, J. M. Fedeli, S. Zlatanovic, H. Youfang, B. P. P. Kuo, E. Myslivets, N. Alic, S. Radic, G. Z. Mashanovich, and G. T. Reed, "50-Gb/s Silicon Optical Modulator," *Photonics Technology Letters, IEEE, Volume 24*, 2012, pp. 234-236.
3. K. Kim, S.-H. Cho, and C.-W. Lee, "Nonlinear optics: Graphene-silicon fusion," *Nat Photon, Volume* 6, 2012, pp. 502-503.
4. A. N. Grigorenko, M. Polini, and K. S. Novoselov, "Graphene plasmonics," *Nat Photon, Volume* **6**, 2012, pp. 749-758.
5. B. Sensale-Rodriguez, R. Yan, M. M. Kelly, T. Fang, K. Tahy, W. S. Hwang, D. Jena, L. Liu, and H. G. Xing, "Broadband graphene terahertz modulators enabled by intraband transitions," *Nat Commun, Volume 3*, 2012, pp. 780,.
6. A .Vakil, N.Engheta."Transformation Optics Using Graphene," *Science, Volume 332,* 2011, p. 1291.
7. R. Hao, W. Du, H. Chen, X. Jin, L. Yang, and E. Li, "Ultra-compact optical modulator by graphene induced electro-refraction effect," *Applied Physics Letters, Volume 103*, 2013, 061116.
8. M. Jablan, H. Buljan, and M. Soljačić, "Plasmonics in graphene at infrared frequencies," *Physical Review B, Volume 80*, 2009, 245435.
9. L. Ju, B. Geng, J. Horng, C. Girit, M. Martin, Z. Hao, H. A. Bechtel, X. Liang, A. Zettl, Y. R. Shen, and F. Wang, "Graphene plasmonics for tunable terahertz metamaterials," *Nat Nano, Volume 6*, 2011, pp. 630-634.
10. Z. H. Ni, H. M. Wang, J. Kasim, H. M. Fan, T. Yu, Y. H. Wu, Y. P. Feng, and Z. X. Shen, "Graphene Thickness Determination Using Reflection and Contrast Spectroscopy," *Nano Letters, Volume 7*, 2007, pp. 2758-2763.